

## ROTATING ELLIPTIC ANALYSERS AND AUTOMATIC ANALYSIS OF POLARISED LIGHT—PART II

BY S. R. RAJAGOPALAN\*

(Department of Chemistry, Indian Institute of Technology, Madras-36)

AND

S. RAMASESHAN, F.A.SC.

(Department of Physics, Indian Institute of Technology, Madras-36)

Received August 17, 1964

### § 1. INTRODUCTION

IN Part I (P-I) of this series the basic principles of analysis of polarised light was discussed. It was pointed out that a rotating elliptic analyser could be used for scanning the Poincaré sphere to achieve automatic analysis. In this part, we shall enumerate a few important rotating elliptic analysers and discuss how they can be used for the analysis of polarised light.

### § 2. DIFFERENT TYPES OF ROTATING ELLIPTIC ANALYSERS

By having a quarterwave plate and a linear analyser each covering the full field of view, we can get a few types of rotating elliptic analysers by rotating one or both of the elements. Such analysers scan the Poincaré sphere along a meridian, a latitude circle or an oblique path (Fig. 1). Rotating elliptic analysers scanning along two different paths can be made from two quarterwave plates each covering one half of the field and a linear analyser. The schematic arrangement and path scanned are shown in Fig. 2. The combination of a quarterwave plate and two linear elements in the two halves of the field of view can be used for obtaining two elliptic analysers scanning along the same path (Fig. 3). These do not exhaust all possible permutations and combinations; but they are the most important ones that can be made from a birefringent element (retardation =  $\pi/2$ ) and a linear analyser. Besides these, we can think of using a stationary variable birefringence element and a rotating linear analyser. All these analysers could be used in methods based on intensity measurement. Some can be used in methods which do not require absolute measurement of intensity.

\* On leave of absence from the Central Electrochemical Research Institute, Karaikudi-3.

### § 3. METHODS OF ANALYSIS BASED ON MEASUREMENT OF ABSOLUTE INTENSITY

#### (a) Automatic and Continuous Measurement of the Stokes Parameters

Continuous measurement of the Stokes parameters ( $I$ ,  $M$ ,  $C$  and  $S$ ) requires that an elliptic analyser be made to scan the Poincaré sphere in such a manner that the transmitted intensities  $I_0$ ,  $I_{45^\circ}$ ,  $I_{90^\circ}$  and  $I_L$  when the analyser is in the states  $H$ ,  $C'$ ,  $V$  and  $L$  are recorded using a suitable timing device. The four intensities are sufficient for specifying the state of the incident light.

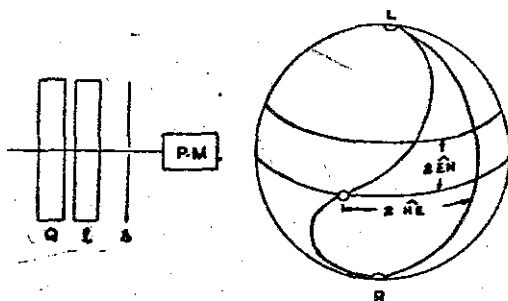


FIG. 1. Q, quarter wave plate;  $l$ , linear element;  $s$ , slit; P.M., photomultiplier tube. The following are the main types of rotating analysers that can be made from the elements shown in the sketch. (a) Q—stationary;  $l$ —rotating; path scanned—a meridian of longitude  $2\widehat{HE}$ . (b) Q—rotating,  $l$ —stationary; path scanned—oblique; (c) Q and  $l$  rotating at different speeds; path scanned—oblique; (d) Q and  $l$  rotating at the same speed; path scanned—a latitude circle of latitude  $2\widehat{EN}$  ( $N$  stands for the vibration direction of the linear element). The angular separation between two directions will be denoted by writing the symbol  $\wedge$  on top of the letters standing for the two directions. Thus, the inclination of the slow axis  $E$ , with reference direction,  $H$  will be represented by  $\widehat{HE}$ .

However, if the intensities  $I_{45^\circ}$  and  $I_R$  corresponding to states  $D$  and  $R$  are also recorded then they serve as a check (see P-I, § 3 a, Fig. 2). From these readings  $I$ ,  $M$ ,  $C$ ,  $S$  and  $\lambda_p$  and  $\omega_p$  are obtained from the following formulae

$$I = I_0 + I_{90^\circ} = I_{45^\circ} + I_{-45^\circ} = I_L + I_R \quad (1)$$

$$M = I_0 - I_{90^\circ} \quad (2)$$

$$C = I_{45^\circ} - I_{-45^\circ} = 2I_{45^\circ} - I \quad (3)$$

$$S = I_L - I_R = 2I_L - I \quad (4)$$

$$\tan 2\lambda_p = \frac{C}{M} \quad (5)$$

These equations are valid whether the light is completely polarised or partially polarised. The equation for  $\omega_p$  is different for completely and partially polarised light. For completely polarised light

$$\sin 2\omega_p = \frac{S}{I} \quad (6)$$

and for partially polarised light

$$\sin 2\omega_p = \frac{S}{Ip} \quad (7)$$

where  $p$  is the degree of polarisation defined by

$$p = \frac{\sqrt{M^2 + C^2 + S^2}}{I} \quad (8)$$

All analysers discussed in § 2 scan the Poincaré sphere in such a manner that they pass through H, V and either C' or L or both. The rotating elliptic analysers 1  $a$ , 1  $b$ , 1  $c$  and 3  $a^*$  pass through H, V and L only and can, therefore directly measure I, M and S; whereas the analysers 1  $d$  and 3  $b$  pass through H, V and C' and hence can measure I, M and C. These analysers which measure I, M and C or S are useful for the analysis of completely polarised light (see P-I § 4).

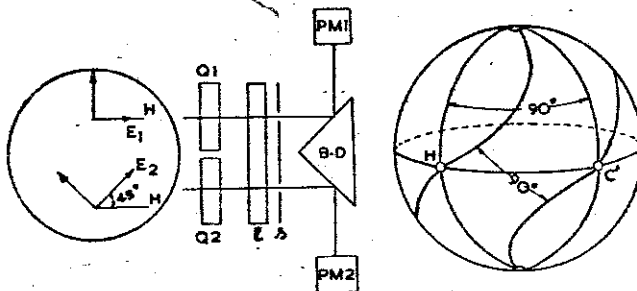


FIG. 2. Two elliptic analysers simultaneously moving along the same path.  $A_1$  and  $A_2$ —two elliptic analysers. (a) Q—stationary,  $l_1$  and  $l_2$  independently rotating in the same direction,  $N_1N_2 = 45^\circ$  path scanned—meridian of longitude zero; (b) Q—rotating at the same speed and in the same direction as  $l_1$  and  $l_2$  which rotate independently,  $N_1N_2 = 45^\circ$ ; path scanned—equatorial circle.

\* These numbers refer to those given in the figure. Hereafter we shall refer to the analysers by the number given to them in the figure.

The analysers 2 *a* and 2 *b* pass through H, V, C' and L and can, therefore, measure all the four Stokes parameters. They are more versatile in the sense that they can analyse both completely and partially polarised light.

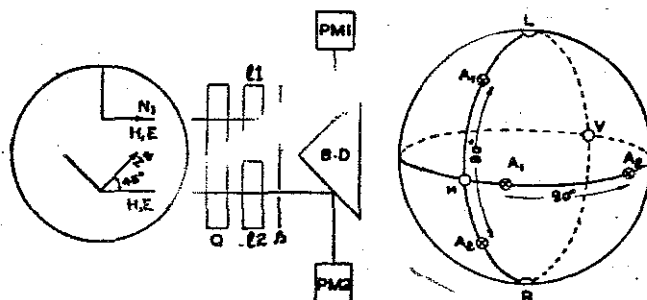


FIG. 3. A rotating elliptic analyser scanning the Poincaré sphere simultaneously along two paths. B.D., beam deflecting prism. (a)  $Q_1, Q_2$ —stationary,  $I$ —rotating,  $\widehat{E}_1 E_2 = 45^\circ$ ; path scanned—Two meridians of longitude zero and  $90^\circ$ ; (b)  $Q_1, Q_2$ —rotating independently,  $I$ , stationary,  $\widehat{E}_1 E_2 = 45^\circ$ ; path scanned—Two oblique paths separated by  $90^\circ$ .

The speed of analysis is half the time taken for one rotation of the revolving component of the rotating elliptic analyser. Excepting the analysers 1 *b* and 2 *b* others can only be rotated by mechanical means and, therefore, the speed of analysis will be about one-eightieth of a second. If the birefringent element of 1 *b* and 2 *b* is an electro-optic cell then, very rapid rotation is possible rendering the analysis of changing states of polarisation feasible.

#### (b) Accuracy of the Stokes Parameters Method

The error in  $\lambda_p$  and  $\omega_p$  are related to the probable errors  $(dR)_1$  and  $(dR)_2$  in the quantities  $C/M$  and  $S/I$  by the following equations (see Appendix I).

$$d\lambda_p = \pm \frac{\cos^2 2\lambda_p (dR)_1}{2} \quad (9)$$

$$d\omega_p = \pm \frac{(dR)_2}{2 \cos 2\omega_p} \quad (10)$$

Archard *et al.* (1952) have found that changes in intensity of the order of  $10^{-3}$  lumen could be measured by a photomultiplier tube. The error in the photoelectric measurement of intensity is generally not dependent on the absolute intensity falling on the photomultiplier tube. If it is assumed that  $dI = \pm 10^{-3}$  lumen,  $I = 10^{-4}$  lumen,  $C = M = 0.5$ ,  $(dR)_1 \approx (dR)_2 \approx \pm 2 \times 10^{-4}$  and if  $\cos^2 2\lambda_p$  takes the maximum value of unity then  $d\lambda_p < 10^{-4}$  rad. ( $\approx 0.006^\circ$ ). If  $S/I = 0.5$  and  $\cos 2\omega_p > 0.1$  then  $10^{-4}$  rad.

$< d\omega_p < 10^{-3}$  rad. ( $\approx 0.06^\circ$ ). This shows that by measuring intensity accurate to one in ten-thousand, the Stokes parameters are obtained with accuracy sufficient to yield values of  $\lambda_p$  and  $\omega_p$  whose accuracy is better than  $\pm 1$  minute of arc.

Though this statement is generally true still there are certain positions of P where the accuracy may be poor. For instance,  $d\lambda_p$  depends upon  $(dR)_1$  which is large if M is small. So if P is close L, R, C' or D the error in  $\lambda_p$  calculated by equation 5 will be large.  $d\omega_p$  depends upon  $\cos 2\omega_p$  and is large if  $\cos 2\omega_p$  is small, i.e., P is near L or R.

It is important to stress that the inaccuracies of the positions of a point arise from two sources, viz., (a) experimental inaccuracies (which is of the order of  $10^{-8}$  lumen in the measurement of intensity) and (b) computing  $\lambda$  and  $\omega$  from experimentally determined values. Depending upon the position of the point on the Poincaré sphere, one can use different formulae to minimise the error due to the second cause. For example, let us consider a point  $P_1$  close to L. This point can be defined in terms of a longitude measured along the equator, HC'VD and a latitude measured from it (Fig. 4). Alternately, the great circle LDRC' could be considered as the equator and the points H and V as poles for specifying the angular co-ordinates of  $P_1$ . If the former is used then the  $\lambda$  and  $\omega$  calculated from 5 and 6 are subject to larger error due to the small value of M and large value of  $\omega$ . By using the latter we make M large and  $\omega$  small and minimise the error. Once the position of  $P_1$  is accurately defined with respect to the poles H and V and the equator LDRC', its position relative to the poles L, R and the equator, HC'VD which is required is easily calculated without loss of accuracy. Explicit expressions for this procedure are given in Appendix II for the cases when P is near L and when it is near C'.

### (c) Application of the Three-Intensity Method

In P-I it was pointed out that the position of P can be fixed by measuring intensities transmitted by three analysers  $A_1$ ,  $A_2$  and  $A_3$  located on two great circles. All the analysers described in § 2 are useful for this method. Among them the analysers 2 a and 2 b appear to hold a greater promise, because in one scanning operation we get all the readings required. Though it is possible to find  $\lambda_p$  and  $\omega_p$  from  $I_1$ ,  $I_2$  and  $I_3$ , the intensities transmitted by any three analysers, it is better to choose two on the same meridian because it simplifies the calculation (see Appendix III).

With an analyser similar to 3 *b* (two analysers scanning along the equator) it becomes possible to find  $\lambda_p$  and  $\omega_p$  by finding the positions  $A_1$  and  $A_2$  at which they transmit the same intensity and by determining the magnitude of the intensity transmitted.

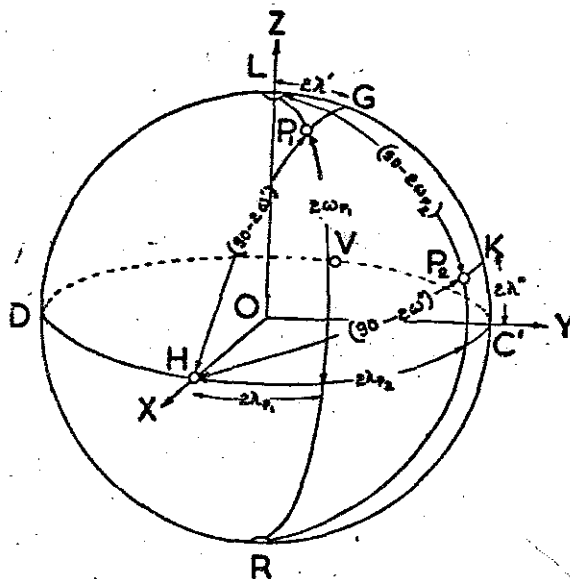


FIG. 4. Geometrical construction illustrating the conclusions of § 3 *b*.

An interesting modification of the analyser 3 *b* is worth mentioning. The optical elements are arranged such that one half of the field of view is covered by a stationary circular analyser and the other half by a rotating elliptic analyser scanning along the equatorial circle. The position  $A_1$  of the rotating analyser at which the sum of the intensities transmitted by the analysers is a maximum is recorded. The azimuth of  $A_1$  gives the azimuth of P (see P-I, § 3 *b*, Fig. 4) and from the intensity  $I_L$  transmitted by the circular analyser  $\omega_p$  can be found with the help of the equation

$$\omega_p = \cos^{-1} \left( \sqrt{\frac{I_L}{I}} \right). \quad (11)$$

When P is close to L or R, it may be rather difficult to locate the position  $A_1$  corresponding to maximum in the value of  $I_L + I_A$  and hence  $\lambda_p$  would be in error. The accuracy can be improved by scanning along  $45^\circ$  latitude circle.

The method so far described requires a knowledge of  $I$  which is easily obtained, by adding the intensities transmitted by the analysers  $H$  and  $V$  or any other two orthogonal analysers.

Calculation of the accuracy of this method shows that if the ratio  $I_A/I$  is measured to an accuracy of  $\pm 10^{-4}$  then the error in  $\lambda_p$  and  $\omega_p$  will be less than a minute of arc. The accuracy of arc length calculated from the ratio  $I_A/I$  is maximum when the ratio is near about 0.5. Hence, the positions of  $A_1$ ,  $A_2$  and  $A_3$  should be so chosen that they transmit nearly half the incident intensity.

#### (d) Method of Extrapolation

A different procedure for finding the position of  $P$  from intensity data will be described briefly next. A rotating elliptic analyser describing an oblique path comes back to the starting point after going round the Poincaré sphere  $n$  times. During each rotation the transmitted intensity passes through a maximum and a minimum. The maxima and minima of successive rotations are different. Thus, the intensity variation with time appears very similar, in form, to the amplitude-modulated wave (Fig. 5). The envelope of intensity vs. time graph, therefore, gives us the variation in the maximum and minimum value over  $n$  rotations round the Poincaré sphere. To locate  $P_0$ , we choose two symmetrical points on either side of the minimum of the envelope. From the time axis the positions  $A_1$  and  $A_2$  of the analysers corresponding to the symmetrical points, chosen are found. The intensity transmitted,  $I_A$ , is also read off. From  $I_A$ ,  $A_1$  and  $A_2$  the position of  $P_0$ , and

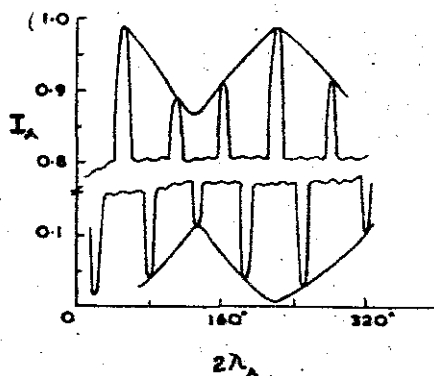


FIG. 5. Theoretically calculated variation of intensity transmitted through the elliptic analyser  $I C$  as it scans the surface of the Poincaré sphere. The following values were assumed for the calculation:  $\omega_p = 25^\circ$ ,  $\lambda_p = 20^\circ$ . Linear element rotates six times faster than the quarterwave plate.

hence  $P$ , is found (see Appendix IV). The accuracy with which the position of  $P$  is found depends on that with which  $A_1$  can be determined. In this regard this method poses difficulties in instrumentation.

#### 4. METHODS THAT DO NOT REQUIRE MEASUREMENT OF ABSOLUTE INTENSITY

##### (a) Method of No Intensity Variation as the Elliptic Analyser Scans the Poincaré Sphere

If the scanning is done along a great circle whose pole is  $P$ , then the transmitted intensity does not exhibit any variations. If this great circle is found then it fixes  $P$  (see P-I, § 3 c). This can be realised with the arrangement shown in Fig. 6. Initially, the electro-optic cell is inactive and the linear analyser which is ganged to the electro-optic cell (EOC) rotates till the transmitted intensity is a minimum and the output of the photocell 1 freezes the movement of  $I_1$ . Simultaneously the EOC and the photocell 2 become active. The output of photocell 2 increases the field strength across the EOC till the intensity transmitted through  $I_2$  does not vary as  $I_2$  rotates, i.e., the incident light  $P$  is brought to the circular state. The longitude  $2\lambda_E$  of the slow axis of the EOC and the retardation  $\delta$  are recorded.  $\lambda_p$  and  $\omega_p$  are then given by

$$\lambda_p = \lambda_E - \frac{\pi}{4} \quad \text{and} \quad |2\omega_p| = \frac{\pi}{2} - \delta. \quad (12)$$

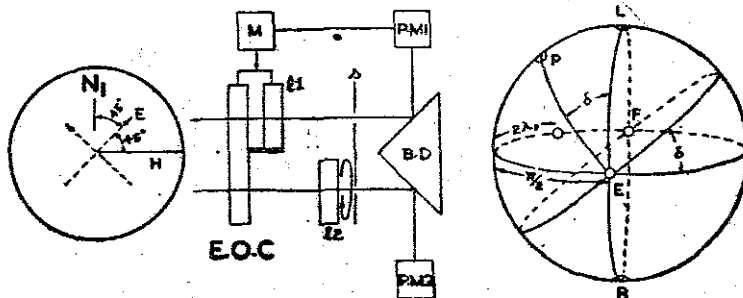


FIG. 6. EOC, Electro-optic cell;  $I_1$ , linear analyser ganged to EOC. The vibration direction of  $I_1$  is at  $\pm \pi/4$  to the field in EOC.

The arrangement discussed can be made to analyse slowly changing states of polarisation by adjusting the circuitry in such a manner that the moment there are fluctuations in the output of photocell 2, photocell 1 is commissioned which again searches the position of minimum intensity and thus the process repeats. This method is in principle the same as the method of Kent and Lawson (1937).



Instead of setting the axes of the birefringent medium  $\pm \pi/4$  to those of the incident elliptic vibration one can cause the ellipse to turn, by altering the polariser azimuth, till its axes are  $\pm \pi/4$  to the axes of the birefringent element. It may not always be feasible to alter the polariser azimuth and hence this method is of limited application.

(b) *Null Method*

In the null method the analyser is made to coincide with  $P_a$ ; whether the coincidence has occurred or not being judged by the transmitted intensity. Before we start to discuss this method it is necessary to digress a little and consider the form of the locus of  $I_{\min.}$  when the scanning is done along latitudes and meridians. The line joining  $I_{\min.}$  of various latitudes is a meridian passing through  $P_a$ . In the case of scanning along a meridian, the point where  $I_A$  is minimum should satisfy the relation

$$\tan 2\omega_p = \cos 2(\lambda_p - \lambda_A) \tan 2\omega_A \quad (13)$$

where  $\omega_A$  and  $\lambda_A$  stand, respectively, for the ellipticity and azimuth of the analyser. The locus of  $I_{\min.}$  for various meridians is an odd-shaped curve, which is schematically shown in Fig. 7. Each point on this locus satisfies the above relation.

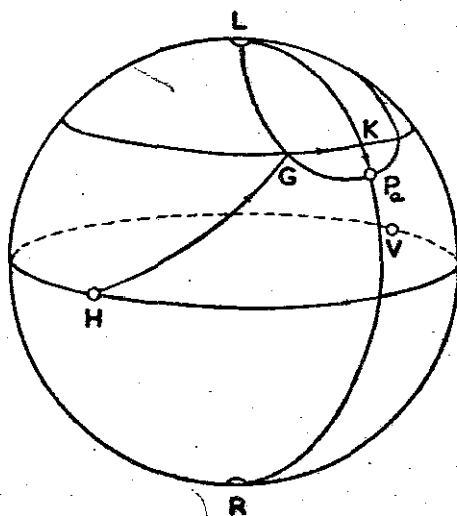


FIG. 7. Path taken by the analyser while hunting  $P_a$ .

To automatically reach the point  $P_a$  we must employ a rotating elliptic analyser in which both the elements are rotated, for example, analyser 1  $c$ . Perhaps the one method of making 1  $c$  reach the point  $P_a$  from H is to have a programmer and make the elements rotate at different speeds till the transmitted intensity becomes a minimum, i.e., analyser has reached G (Fig. 7). Then the elements are made to rotate with the same velocity till the transmitted intensity is again a minimum. Now the analyser is at K. The programmer now stops the movement of the birefringent plate and the linear analyser rotates till the transmitted intensity is zero. When this happens the linear analyser also stops and the state  $P_a$  of the analyser is recorded.

### § 5. SUMMARY

The various main arrangements leading to a few typical rotating elliptic analysers are discussed. Simple devices for the determination of I, M, C, S of completely and partially polarised light beams are given. The possibility of using a rotating elliptic analyser having an electro-optic cell, for the determination of the Stokes parameters of light beams whose state of polarisation is rapidly changing is pointed out. The accuracy of the Stokes parameter method is analysed and it is found that this method leads to  $\lambda_p$  and  $\omega_p$  values which are subject to an error smaller than one minute of arc (intensity measurement accurate to one in ten thousand). Some of the other methods of using the rotating elliptic analysers are also discussed. It is pointed out that the Stokes parameter method and the interference method, using the concept that orthogonal states do not interfere, are the most promising methods for the analyses of polarised light.

### § 6. ACKNOWLEDGEMENT

The authors thank Prof. M. V. C. Sastri, Head of the Department of Chemistry, for his interest. One of us (S. R. R.) is thankful to the Council of Scientific and Industrial Research for granting leave.

### § 7. REFERENCES

1. Archard, Clegg and Taylor *Proc. Phys. Soc. London*, 1952, 65 B, 758.
2. Kent and Lawson .. *J. Opt. Soc. Am.*, 1937, 27, 117.
3. Mellor .. *Higher Mathematics for Students of Physics and Chemistry*. Dover Publications, 1955.
4. P-I Rajagopalan and Ramaseshan "Rotating elliptic analysers and automatic analysis of polarised light—Part I, *Proc. Ind. Acad. Sci.*, 1964, 60 A, 297-310.
5. Todhunter and Leahey .. *Spherical Trigonometry*, Macmillan and Co., Ltd., London, 1907.

## APPENDIX I

### *Accuracy of the Stokes Parameter Method*

The component of the Stokes vector,  $S$ , along any direction  $C$  is equal to the difference in the intensities transmitted by the orthogonal analysers  $C$  and  $-C$ .

$$S = I_C - I_{-C} \quad (I.1)$$

If the error in measurement of intensity is  $\pm dI$  the probable error  $dS$  in  $S$  is given by (Mellor, 1955, pp. 527-29)

$$dS = \pm \sqrt{2} (dI) \quad (I.2)$$

$dI$  does not depend on  $I$  and hence  $dS$  is independent of  $|S|$ . Therefore, the probable error ( $dR$ ), in the ratio  $C/M$  is

$$(dR)_1 = \pm \frac{\sqrt{\left(\frac{C \cdot dS}{M}\right)^2 + (dS)^2}}{M} \quad (I.3)$$

Substituting  $R_1$  for  $C/M$  in equation 5 (see § 3) and differentiating we get

$$d\lambda_p = \frac{\cos^2 2\lambda_p (dR)_1}{2} \quad (I.4)$$

In the same way the probable error ( $dR$ )<sub>2</sub> in  $S/I$  is

$$(dR)_2 = \pm \frac{\sqrt{\left(\frac{S \cdot dS}{I}\right)^2 + (dI)^2}}{I} \quad (I.5)$$

Setting  $S/I = R_2$  and differentiating equation 6 (see § 3) we get

$$d\omega_p = \pm \frac{(dR)_2}{2 \cos 2\omega_p} \quad (I.6)$$

## APPENDIX II

We shall evolve here a method for calculating without loosing accuracy,  $\lambda$  and  $\omega$  of states close to L (or R) and C' (or D) from the Stokes parameters. Let us consider  $P_1$  close to L. Let us consider H and V as poles and the great circle DRC'L as equator (Fig. 4). Then P is defined by the longitude  $2\lambda'$  (measured on DRC'L) and latitude  $2\omega'$  (measured from DRC'L). These can be calculated from the Stokes parameters by using the relations

$$\tan 2\lambda' = \frac{C}{S} \quad (\text{II.1})$$

$$\sin 2\omega' = \frac{M}{I} \quad (\text{II.2})$$

As S is large, the error in  $\lambda'$  is small and the accuracy of  $\omega'$  is good since  $2\omega'$  is small.

From  $\lambda'$  and  $\omega'$ ,  $\lambda_{p_1}$  and  $\omega_{p_1}$  are obtained by solving the right-angled spherical triangle  $LP_1G$  (Fig. 4). In this triangle we know

$$P_1\hat{G}L = 90^\circ, \quad \widehat{P_1G} = 2\omega', \quad \widehat{LG} = 2\lambda'$$

therefore,

$$\cos \widehat{LP_1} = \cos (90 - 2\omega_{p_1}) = \sin 2\omega_{p_1} = \cos 2\omega' \cos 2\lambda' \quad (\text{II.3})$$

and

$$\begin{aligned} \cos (90 - 2\lambda_{p_1}) &= \sin 2\lambda_{p_1} = \tan 2\lambda' \cot (90 - 2\omega_{p_1}) \\ &= \tan 2\lambda' \tan 2\omega_{p_1}. \end{aligned} \quad (\text{II.4})$$

Consider the point  $P_2$  close to C'. As before the point  $P_2$  can be specified by the longitude  $2\lambda''$  and latitude  $2\omega''$  (Fig. 4). These are calculated from the Stokes parameters by the equations

$$\tan 2\lambda'' = \frac{S}{C} \quad (\text{II.5})$$

$$\sin 2\omega'' = \frac{M}{I} \quad (\text{II.6})$$

Since  $C$  is large, the error in  $\lambda''$  is small.  $\omega''$  is small and hence the error in  $\omega''$  is small.

From  $\lambda''$  and  $\omega''$ ,  $\lambda_{p_1}$  and  $\omega_{p_1}$  are readily found by solving the spherical triangle  $LP_2K$ .

In this triangle we know that

$$\widehat{L\hat{K}P_2} = 90^\circ, \quad \widehat{P_2K} = 2\omega'', \quad \widehat{LK} = (90 - 2\lambda'')$$

therefore,

$$\cos \widehat{LP_2} = \cos (90 - 2\omega_{p_1}) = \sin 2\omega_{p_1} = \cos 2\omega'' \sin 2\lambda'' \quad (\text{II.7})$$

$$\begin{aligned} \sin (90 - 2\lambda_{p_1}) &= \cos 2\lambda_{p_1} \\ &= \frac{\sin 2\omega''}{\sin (90 - 2\omega_{p_1})} = \frac{\sin 2\omega''}{\cos 2\omega_{p_1}}. \end{aligned} \quad (\text{II.8})$$

If the point is nearer  $R$  or  $D$ ,  $\lambda_p$  and  $\omega_p$  can be obtained, without loss of accuracy, by a similar procedure.

### APPENDIX III

Let the fraction transmitted by  $A_1$ ,  $A_2$  and  $A_3$  be  $I_1/I$ ,  $I_2/I$  and  $I_3/I$  respectively. Let  $A_1$ ,  $A_2$  lie on one meridian and  $A_3$  on another (Fig. 8).

By a theorem in spherical trigonometry (see Art. 145, Todhunter and Leathem, 1907) we have

$$\cos \widehat{PA_2} \sin \widehat{A_1L} + \cos \widehat{PA_1} \sin \widehat{LA_2} + \cos \widehat{PL} \sin \widehat{A_2A_1} = 0. \quad (\text{III.1})$$

But

$$\widehat{LA_2} = -\widehat{A_2L}$$

and

$$\widehat{PL} = (90 - 2\omega_p)$$

$$\therefore \cos(90 - 2\omega_p)$$

$$= \sin 2\omega_p = \frac{\cos \widehat{PA_2} \sin \widehat{A_1L} - \cos \widehat{PA_1} \sin \widehat{A_2L}}{\sin \widehat{A_2A_1}}. \quad (\text{III.2})$$

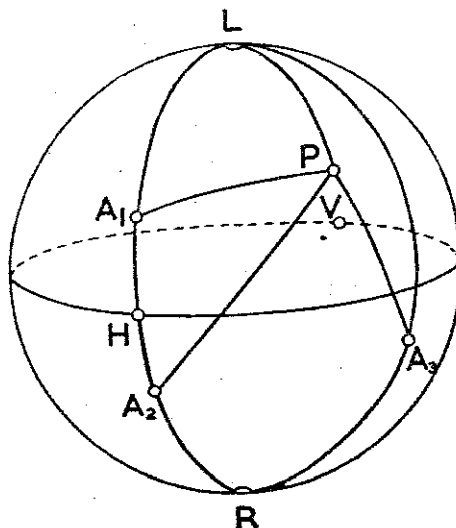


FIG. 8. Geometrical construction for the formula derived in Appendix III.

To find the azimuth of P the spherical triangles  $LA_1P$  and  $LPA_2$  are to be solved. Since all the sides are known we have

$$\cos A_1 \hat{L}P = \frac{\cos \widehat{PA_1} - \cos \widehat{A_1L} \cos \widehat{PL}}{\sin \widehat{A_1L} \sin \widehat{PL}} \quad (\text{III.3})$$

and

$$\cos \widehat{PLA_2} = \frac{\cos \widehat{PA_2} - \cos \widehat{A_2L} \cos \widehat{PL}}{\sin \widehat{A_2L} \sin \widehat{PL}} \quad (\text{III.4})$$

If  $2\lambda_{A_1}$  and  $2\lambda_{A_2}$  are the longitudes of  $A_1$  and  $A_2$  then

$$2\lambda_{A_1} \pm A_1 \hat{L}P = 2\lambda_{A_2} \pm A_2 \hat{L}P = 2\lambda_P \quad (\text{III.5})$$

The equations III.1 to III.4 can be written in terms of the experimentally measured quantities by making the following substitutions:

$$\widehat{PA_1} = 2 \cos^{-1} \sqrt{\frac{I_1}{I}}, \quad \widehat{PA_2} = 2 \cos^{-1} \sqrt{\frac{I_2}{I}}, \quad \widehat{PA_3} = 2 \cos^{-1} \sqrt{\frac{I_3}{I}}$$

$$\widehat{A_1L} = (90 - 2\omega_{A_1}); \quad \widehat{A_2L} = (90 - 2\omega_{A_2}); \quad \widehat{A_1A_2} = 2(\omega_{A_1} - \omega_{A_2})$$

$$\widehat{A_3L} = (90 - 2\omega_{A_3}).$$

The calculations can be simplified still further if one of the analysers say  $A_2$  is L because  $\omega_P$  is then straightaway obtained from the fraction of the intensity transmitted by L. But it would lead to a large error, if  $\widehat{PL}$  is less than  $50^\circ$ .

## APPENDIX IV

Let us assume that the quarterwave plate rotates slower than the linear analyser. The minimum of the envelope corresponds to the intensity transmitted by the analyser when it is nearest to the point  $P_a$ . Therefore, the positions  $A_1$  and  $A_2$  of the analyser are also near  $P_a$ . Since they transmit equal intensity they are on the same small circle drawn around  $P_a$ . The path traversed by the analyser is nearly a meridian. Therefore,  $A_1$  and  $A_2$  may be looked upon as points of tangential contact between the meridians passing through  $A_1$  and  $A_2$  and the small circle whose centre is at  $P_a$  and radius  $2 \cos^{-1} \sqrt{I_{A_1}/I}$ , where  $I_{A_1}$  is the intensity transmitted by  $A_1$  and is equal to that transmitted by  $A_2$  (Fig. 9). Therefore the spherical triangles  $LP_aA_2$  and  $LP_aA_1$  are right-angled triangles; the angles  $P_a\hat{A}_1L$  and  $P_a\hat{A}_2L$  are right angles.

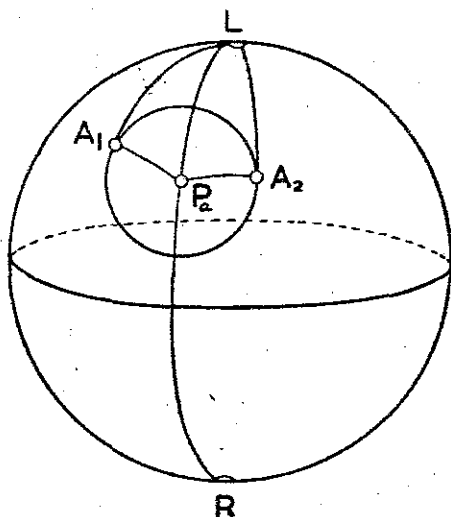


FIG. 9. Geometrical construction for the formula derived in Appendix IV.

Since  $\widehat{P_aA_2}$  and  $\widehat{LA_2}$  are known we can calculate  $\widehat{LP_a}$  ( $= 90 - 2\omega_{P_a}$ ) by the formula.

$$\cos \widehat{LP_a} = \cos (90 - 2\omega_{P_a}) = \cos 2\omega_{P_a} = \cos \widehat{P_aA_2} \cos \widehat{LA_2}. \quad (\text{IV.1})$$



The angles  $P_a \widehat{L}A_1$  is equal to  $2(\lambda_p - \lambda_{a_1})$  and is given by

$$\sin P_a \widehat{L}A_1 = \frac{\sin \widehat{P_a A_1}}{\sin \widehat{L P_a}} \quad (\text{IV.2})$$

These equations can be written in terms of experimentally measured quantities by making the following substitutions

$$\widehat{P_a A_1} = \widehat{P_a A_2} = 2 \cos^{-1} \sqrt{\frac{I_{A_2}}{I}}; \quad \widehat{L}A_1 = (90 - 2\omega_{a_1})$$

$$\widehat{L}A_2 = (90 - 2\omega_{a_2}).$$